IJCSE International Journal of Computer Sciences and Engineering Open Access
Research Paper Vol.-6, Issue-6, June 2018 E-ISSN: 2347-2693

Numerical Simulation of Soret-Dufour and Radiation effects on Unsteady MHD flow of Viscoelastic Dusty fluid over Inclined Porous Plate

N. Pandya[1] and R. K. Yadav[2*]

[1,2]Department of Mathematics and Astronomy, University of Lucknow, Lucknow-226007, India

[*]*Corresponding Author: ravikant.yadav31@gmail.com*

Available online at: www.ijcseonline.org

Accepted: 15/Jun/2018, Published: 30/Jun/2018

Abstract . The purpose of this paper is to present a numerical analysis of an unsteady three dimensional MHD flow of dusty fluid past an infinite inclined porous plate. The Thermal diffusion (Soret), Diffusion thermo (Dufour) and radiation effects on natural convection heat and mass transfer of viscoelastic fluid over a fixed inclined porous plate are presented. The governing non-linear partial differential equations are transformed into a system of partial differential equations using similarity transformations. After transformation the resulting equations are then solved numerically by the use of Crank-Nicolson implicit finite difference method. Profiles of dimensionless velocity, temperature and concentration are shown graphically for various values physical parameter like Prandtl number , Schmidt number , magnetic parameter , Hall parameter , Soret number, Dufour number, Viscoelastic parameter radiation parameter, time , permeability parameter , dusty fluid parameter , dust particle parameter , thermal Grashof number , solutal Grashof number , inclination angle . Skin friction coefficient, Nusselt number and Sherwood number are discussed with help of tables.

Keywords— Free convection, MHD flow, Dusty fluid, Viscoelastic fluid, Radiation effect, Heat and Mass transfer, Soret-Dufour effects, Crank-Nicolson finite difference method.

MSC 2010 Codes --76A10, 76W05, 80A20, 78A40, 80M20

I. INTRODUCTION

In recent years, the MHD(Magnetohydrodynamics) flow of viscous or viscoelastic fluid through porous media is attracting towards itself due to it's quite prevalent in nature. There are many viscoelastic fluids that cannot be characterized by Maxwell's or Oldroyd's constitutive relations. One such fluid is Walters' (model B) viscoelastic fluid which is used in biotechnology and industry. The problems of the fluid dynamics involving dust, gas particles mixture arise in many processes of practical importance. The effect of dust particles on the viscoelastic fluid flow has many applications as in the production of plastic products like rayon and nylon, in the purification of crude oil, in the pulp and paper industry, in the textile industry, in treating environment pollution, in the petroleum industry, in the purification of rain water etc.

Many authors have carried out the investigation of dusty viscoelastic fluids under different conditions. Walters [1] proposed a theoretical model for elastoviscous fluids. Rana and Sharma [2] discussed

the thermosolutal instability of Walters' (model B) viscoelastic rotating fluid permeated with suspended particles and variable gravity field in porous medium. Dholey et al. [3] analyzed the steady two dimensional stagnation point flow of a walter's-B fluid along a flat deformable stretching surface. N. pandya and A. K. Shukla [4] studied effect of radiation and chemical reaction on an unsteady Walter's-B viscoelastic MHD flow past a vertical porous plate. Pradeep Kumar [5] investigated instability in Walters B' Viscoelastic Dusty Fluid through Porous Medium. Mahapatra et al. [6] analysed an analytical solution of MHD flow of two visco-elastic fluids over a sheet shrinking with quadratic velocity. Jena et al. [7] studied chemical reaction effect on MHD viscoelastic fluid flow over a vertical stretching sheet with heat source/sink. Manoj et al. [8] investigated heat and mass transfer effects on MHD viscoelastic fluid over a stretching sheet through porous medium in presence of chemical reaction. N. pandya and A. K. Shukla [9] studied effects of thermophoresis, Dufour, Hall and radiation on an unsteady MHD flow past an inclined plate with viscous dissipation.

The objective of this paper to examine the Soret- Dufour and radiation effects on natural convection heat and mass transfer of viscoelastic fluid over a fixed inclined porous plate are presented. The governing non-linear partial differential equations are transformed into a system of partial differential equations using similarity transformations. The resulting equations are then solved numerically using Crank-Nicolson

implicit finite difference method. Profiles of dimensionless velocity, temperature and concentration are shown graphically for various values physical parameter. Skin friction coefficient, Nusselt number and Sherwood number are discussed with help of tables.

II. MATHEMATICAL ANALYSIS

An unsteady MHD flow of dusty fluid past an inclined porous fixed plate in presence of Soret-Dufour effect, Hall effect and radiation effect are considered. x' -axis is considered along plate, y'-axis is perpendicular to it and z'-axis is normal to x'y' plane. A uniform magnetic field B_0 is taken along y'-axis and plate is considered non-electric conducting. In beginning plate and fluid are at same temperature T'_∞ and concentration C'_∞ . For t'> 0, temperature and concentration increase exponentially with time. Magnetic Reynolds number is smaller than transversely applied magnetic field so induced magnetic field is negligible, Cowling[10].

$$J'_x = \frac{\sigma B_0}{1+m^2}(mu'-w')$$
$$J'_z = \frac{\sigma B_0}{1+m^2}(u'+mw') \quad (1)$$

where u' and w' are velocities, J'_x and J'_z are electric current density along x'-axis and z'-axis respectively, m is Hall parameter.

Because of infinite length in x' direction, flow variables are function of t' and y' only. Under usual Boussinesq approximation, governing equations of this model are given by:

$$\frac{\partial v'}{\partial y'} = 0 \Rightarrow v' = -v_0 (const) \quad (2)$$

$$\frac{\partial u'}{\partial t'} + v'\frac{\partial u'}{\partial y'} = \nu \frac{\partial^2 u'}{\partial y'^2} - \nu_1 \frac{\partial^3 u'}{\partial y'^2 \partial t'} + g\beta(T'-T'_\infty)\cos(\alpha)$$
$$+ g\beta^*(C'-C'_\infty)\cos(\alpha) - \frac{\sigma B_0^2}{\rho(1+m^2)}(u'+mw')$$
$$- \frac{\nu u'}{K'} + \frac{KN_0}{\rho}(u'_d - u') \quad (3)$$

$$\frac{\partial w'}{\partial t'} + v'\frac{\partial w'}{\partial y'} = \nu \frac{\partial^2 w'}{\partial y'^2} - \nu_1 \frac{\partial^3 w'}{\partial y'^2 \partial t'}$$
$$+ \frac{\sigma B_0^2}{\rho(1+m^2)}(mu'-w') - \frac{\nu w'}{K'} + \frac{KN_0}{\rho}(w'_d - w') \quad (4)$$

$$m_1 \frac{\partial u'_d}{\partial t'} = S_k (u'-u'_d) \quad (5)$$

$$m_1 \frac{\partial w'_d}{\partial t'} = S_k (w'-w'_d) \quad (6)$$

$$\rho c_p \left(\frac{\partial T'}{\partial t'} + v'\frac{\partial T'}{\partial y'} \right) = k\frac{\partial^2 T'}{\partial y'^2} - \frac{\partial q_r}{\partial y'} + \frac{\rho D_m K_T}{c_s}\frac{\partial^2 C'}{\partial y'^2} \quad (7)$$

$$\frac{\partial C'}{\partial t'} + v'\frac{\partial C'}{\partial y'} = D_m \frac{\partial^2 C'}{\partial y'^2} + \frac{D_m K_T}{T_m}\frac{\partial^2 T'}{\partial y'^2} \quad (8)$$

where S_k is the stoke's resistance coefficient, ν_1 is viscoelasticity, N_0 is the number density of the dust particles which is constant, m_1 is the mass of dust particles, K is the proportionality constant, u'_d and w'_d are the velocity of dust particles along x'-axis and y'-axis respectively, β^* is coefficient of volume expansion for mass transfer, β is volumetric coefficient of thermal expansion, v' is velocity along y'-axis, K' is permeability of porous medium, σ is electrical conductivity, D_m is molecular diffusivity, g is acceleration due to gravity, K_T is thermal diffusion ratio, μ is viscosity, ρ is fluid density, k is thermal conductivity of fluid, C' and T' are dimensional concentration and temperature, C'_∞ and T'_∞ are concentration and temperature of free stream, c_p is specific heat at constant pressure, q_r is radiative heat along y'-axis, ν is kinematic viscosity and T_m is mean fluid temperature.

Boundary and initial conditional for this model are given as:

$$t' \le 0 \quad u'=0 \quad w'=0 \quad u'_d=0 \quad w'_d=0 \quad T'=T'_\infty \quad C'=C'_\infty \quad \forall y'$$
$$t'>0 \quad u'=u_0 \quad w'=0 \quad u'_d=u_0 \quad w'_d=0 \quad T'=T'_\infty+(T'_w-T'_\infty)e^{-At'}$$
$$C'=C'_\infty+(C'_w-C'_\infty)e^{-At'} \quad at\ y'=0$$
$$u'=0 \quad w'=0 \quad u'_d=0 \quad w'_d=0 \quad T'\to T'_\infty \quad C'\to C'_\infty \quad y'\to\infty \quad (9)$$

where T'_w and C'_w are concentration and temperature respectively of plate and $A = \frac{v_0^2}{\nu}$.

The radiative heat flux term after using the Roseland approximation is given by

$$q_r = -\frac{4\sigma}{3k_m}\frac{\partial T'^4}{\partial y'} \tag{10}$$

where σ and k_m are Stefan Boltzmann constant and mean absorption coefficient respectively. in this problem temperature difference within flow is very small, so that T'^4 may be expressed linearly with temperature. It is observed by expanding in a Taylor's series about T_∞' and considering negligible higher order term, hence

$$T'^4 \cong 4T_\infty'^3 T' - 3T_\infty'^4 \tag{11}$$

so, by equations (10) and (11), equation (7) is reduced

$$\rho c_p\left(\frac{\partial T'}{\partial t'} + v'\frac{\partial T'}{\partial y'}\right) = k\frac{\partial^2 T'}{\partial y'^2} + \frac{16\sigma T_\infty'^3}{3k_m}\frac{\partial^2 T'}{\partial y'^2} + \frac{\rho D_m K_T}{c_s}\frac{\partial^2 C'}{\partial y'^2} \tag{12}$$

In order to obtain non dimensional form of governing equations, we introduce following quantities:

$$u = \frac{u'}{u_0},\quad t = \frac{t'v_0^2}{\nu},\quad \theta = \frac{T'-T'_\infty}{T'_w - T'_\infty},$$

$$C = \frac{C'-C'_\infty}{C'_w - C'_\infty},\quad Gm = \frac{\nu g\beta^*(C'_w - C'_\infty)}{u_0 v_0^2}$$

$$Gr = \frac{\nu g\beta(T'_w - T'_\infty)}{u_0 v_0^2},\quad Du = \frac{D_m K_T (C'_w - C'_\infty)}{c_s c_p \nu (T'_w - T'_\infty)},$$

$$Sr = \frac{D_m K_T (T'_w - T'_\infty)}{T_m \nu (C'_w - C'_\infty)}$$

$$K = \frac{v_0^2 K'}{\nu^2},\quad \Pr = \frac{\mu c_p}{k},\quad M = \frac{\sigma B_0^2 \nu}{\rho v_0^2},$$

$$R = \frac{4\sigma T'^3_\infty}{k_m k},\quad Sc = \frac{\nu}{D_m}, \Gamma = \frac{v_0^2 v_1}{\nu^2}$$

$$y = \frac{y'v_0}{\nu},\quad w = \frac{w'}{u_0},\quad u_d = \frac{u'_d}{u_0},$$

$$w_d = \frac{w'_d}{u_0},\quad B = \frac{\nu S_k N_0}{\rho u_0^2},\quad B_1 = \frac{m_1 v_0^2}{\nu S_k} \tag{13}$$

By introducing above dimensionless variables and constants the Equations (3) (6), (8) and (12) converted as follows

$$\frac{\partial u}{\partial t} - \frac{\partial u}{\partial y} = \frac{\partial^2 u}{\partial y^2} - \Gamma\frac{\partial^3 u}{\partial y^2 \partial t} + GrCos(\alpha)\theta$$
$$+GmCos(\alpha)C + B_1(u_d - u) - \left(\frac{M}{1+m^2} + \frac{1}{K}\right)u \tag{14}$$
$$-\left(\frac{mM}{1+m^2}\right)w$$

$$\frac{\partial w}{\partial t} - \frac{\partial w}{\partial y} = \frac{\partial^2 w}{\partial y^2} - \Gamma\frac{\partial^3 w}{\partial y^2 \partial t}$$
$$+B_1(w_d - w) - \left(\frac{M}{1+m^2} + \frac{1}{K}\right)w + \left(\frac{mM}{1+m^2}\right)u \tag{15}$$

$$B\frac{\partial u_d}{\partial t} = u - u_d \tag{16}$$

$$B\frac{\partial w_d}{\partial t} = w - w_d \tag{17}$$

$$\frac{\partial \theta}{\partial t} - \frac{\partial \theta}{\partial y} = \frac{1}{\Pr}\left(1 + \frac{4R}{3}\right)\frac{\partial^2 \theta}{\partial y^2} + Du\frac{\partial^2 C}{\partial y^2} \tag{18}$$

$$\frac{\partial C}{\partial t} - \frac{\partial C}{\partial y} = \frac{1}{Sc}\frac{\partial^2 C}{\partial y^2} + Sr\frac{\partial^2 \theta}{\partial y^2} \tag{19}$$

non dimensional boundary and initial conditions are:

$$t \le 0 \quad u = 0 \quad w = 0 \quad u_d = 0 \quad w_d = 0 \quad \theta = 0 \quad C = 0 \quad \forall y$$
$$t > 0 \quad u = 0 \quad w = 0 \quad u_d = 0 \quad w_d = 0 \quad \theta = e^{-t} \quad C = e^{-t} \quad at\ y = 0$$
$$u = 0 \quad w = 0 \quad u_d = 0 \quad w_d = 0 \quad \theta \to 0 \quad C \to 0 \quad y \to \infty \tag{20}$$

Now, many investigators have interest to calculate physical quantities skin-friction coefficients τ_1 and τ_2 along wall x-axis and z-axis respectively, Nusselt number Nu and Sherwood number Sh. Non-dimensional form of these physical quantities are:

$$\tau_1 = \left(\frac{\partial u}{\partial y}\right)_{y=0}$$

$$\tau_2 = \left(\frac{\partial w}{\partial y}\right)_{y=0}$$

$$Nu = -\left(\frac{\partial \theta}{\partial y}\right)_{y=0}$$

$$Sh = -\left(\frac{\partial C}{\partial y}\right)_{y=0} \quad (21)$$

III. METHOD OF SOLUTION

Nonlinear coupled partial differential Equations 14-19 with conditions 20 are solved by using Crank-Nicolson implicit finite-difference scheme. Consider a rectangular region with y varying from 0 to y max (= 4), where y max corresponds to y = ∞ at which lies well outside the momentum and energy boundary layers. According to Crank- finite-difference equations corresponding to 14-19 are given by

$$\frac{u_{i,j+1}-u_{i,j}}{\Delta t} - \frac{u_{i+1,j}-u_{i,j}}{\Delta y}$$
$$= \left(\frac{u_{i-1,j}-2u_{i,j}+u_{i+1,j}+u_{i-1,j+1}-2u_{i,j+1}+u_{i+1,j+1}}{2(\Delta y)^2}\right)$$
$$-\Gamma\left(\frac{u_{i-1,j}-2u_{i,j}+u_{i+1,j}+u_{i-1,j+1}-2u_{i,j+1}+u_{i+1,j+1}}{2(\Delta y)^2\,\Delta t}\right)$$
$$+B_1\left(\left(\frac{(u_d)_{i,j+1}+(u_d)_{i,j}}{2}\right)-\left(\frac{u_{i,j+1}+u_{i,j}}{2}\right)\right)$$
$$+Gr\cos(\alpha)\left(\frac{\theta_{i,j+1}+\theta_{i,j}}{2}\right)$$
$$+Gr\cos(\alpha)\left(\frac{C_{i,j+1}+C_{i,j}}{2}\right)$$
$$-\left(\frac{M}{1+m^2}+\frac{1}{K}\right)\left(\frac{u_{i,j+1}+u_{i,j}}{2}\right)-\left(\frac{mM}{1+m^2}\right)\left(\frac{w_{i,j+1}+w_{i,j}}{2}\right)$$

$$\frac{w_{i,j+1}-w_{i,j}}{\Delta t} - \frac{w_{i+1,j}-w_{i,j}}{\Delta y}$$
$$= \left(\frac{w_{i-1,j}-2w_{i,j}+w_{i+1,j}+w_{i-1,j+1}-2w_{i,j+1}+w_{i+1,j+1}}{2(\Delta y)^2}\right)$$
$$-\Gamma\left(\frac{w_{i-1,j}-2w_{i,j}+w_{i+1,j}+w_{i-1,j+1}-2w_{i,j+1}+w_{i+1,j+1}}{2(\Delta y)^2\,\Delta t}\right)$$
$$+B_1\left(\left(\frac{(w_d)_{i,j+1}+(w_d)_{i,j}}{2}\right)-\left(\frac{w_{i,j+1}+w_{i,j}}{2}\right)\right)$$
$$-\left(\frac{M}{1+m^2}+\frac{1}{K}\right)\left(\frac{w_{i,j+1}+w_{i,j}}{2}\right)+\left(\frac{mM}{1+m^2}\right)\left(\frac{u_{i,j+1}+u_{i,j}}{2}\right) \quad (22)$$

$$B\left(\frac{(u_d)_{i,j+1}-(u_d)_{i,j}}{\Delta t}\right)=\left(\left(\frac{u_{i,j+1}+u_{i,j}}{2}\right)-\left(\frac{(u_d)_{i,j+1}+(u_d)_{i,j}}{2}\right)\right) \quad (23)$$

$$B\left(\frac{(w_d)_{i,j+1}-(w_d)_{i,j}}{\Delta t}\right)=\left(\left(\frac{w_{i,j+1}+w_{i,j}}{2}\right)-\left(\frac{(w_d)_{i,j+1}+(w_d)_{i,j}}{2}\right)\right) \quad (24)$$

$$\frac{\theta_{i,j+1}-\theta_{i,j}}{\Delta t} - \frac{\theta_{i+1,j}-\theta_{i,j}}{\Delta y} =$$
$$\frac{1}{\Pr}\left(1+\frac{4R}{3}\right)\left(\frac{\theta_{i-1,j}-2\theta_{i,j}+\theta_{i+1,j}+\theta_{i-1,j+1}-2\theta_{i,j+1}+\theta_{i+1,j+1}}{2(\Delta y)^2}\right)$$
$$+Du\left(\frac{C_{i-1,j}-2C_{i,j}+C_{i+1,j}+C_{i-1,j+1}-2C_{i,j+1}+C_{i+1,j+1}}{2(\Delta y)^2}\right) \quad (25)$$

$$\frac{C_{i,j+1}-C_{i,j}}{\Delta t} - \frac{C_{i+1,j}-C_{i,j}}{\Delta y} =$$
$$\frac{1}{Sc}\left(\frac{C_{i-1,j}-2C_{i,j}+C_{i+1,j}+C_{i-1,j+1}-2C_{i,j+1}+C_{i+1,j+1}}{2(\Delta y)^2}\right)$$
$$+Sr\left(\frac{\theta_{i-1,j}-2\theta_{i,j}+\theta_{i+1,j}+\theta_{i-1,j+1}-2\theta_{i,j+1}+\theta_{i+1,j+1}}{2(\Delta y)^2}\right) \quad (26)$$

initial and boundary conditions are also expressed as:

$$u_{i,0}=0 \;\; w_{i,0}=0 \;\; (u_d)_{i,0}=0 \;\; (w_d)_{i,0}=0 \;\; \theta_{i,0}=0 \;\; C_{i,0}=0 \;\; \forall i$$
$$u_{0,j}=0 \;\; w_{0,j}=0 \;\; (u_d)_{0,j}=0 \;\; (w_d)_{0,j}=0 \;\; \theta_{0,j}=e^{-j\Delta t} \;\; C_{0,j}=e^{-j\Delta t}$$
$$u_{n,j}=0 \;\; w_{n,j}=0 \;\; (u_d)_{n,j}=0 \;\; (w_d)_{n,j}=0 \;\; \theta_{n,j}\to 0 \;\; C_{n,j}\to 0 \qquad (27)$$

The coefficient appearing in difference equations are treated as constants. The Crank- Nicolson finite-difference equations at every internal nodal point on a particular n-level constitute a tri-diagonal system of equations. These equations are solved by using the Thomas algorithm [11].

IV. RESULT AND DISCUSSION

The numerical values of the velocities , temperature, concentration, skin-friction, Nusselt number and Sherwood number are computed for different values of parameters like Prandtl number Pr , Schmidt number Sc , magnetic parameter M , Hall parameter m , Soret number Sr, Dufour number Du, Viscoelastic parameter Γ radiation parameter R, time t , permeability parameter K , dusty fluid parameter B_1, dust particle parameter B, thermal Grashof number Gr, solutal Grashof number Gm, inclination angle α .

It is observed in figures 1, 2, 21 and 22 that Soret number Sr increases then velocities profile u, w and concentration profile C increase while temperature profile θ decreases. In figures 3, 4 and 25, Schmidt number Sc increases then velocities profile u, w and concentration profile C decrease. It is observed in figures 7 and 8 that magnetic parameter M increases then velocity profile u decreases and w increases. In figure 9, Hall parameter m increases then velocity profile u increases. It is observed in figures 26 and 27 that on increasing viscoelastic parameter Γ velocity profile u increases near wall with good buoyancy effect after some distance from wall u decreases and velocity profile w increases.

On increasing radiation parameter R velocities profile u and w increase in figures 5 and 6. Velocities profile u and w decrease in figures 12, 13, 10, 11 as B_1 and B increase. It is observed in figures 14 and 15 that inclination angle α increases then velocities profile u and w decrease. In figures 16, 17 velocities profile u and w increase as time t increases. On increasing Dufour number Du, temperature profile θ increases in figure 18. Radiation parameter R increases temperature profile increases in figure 20 while concentration profile C decreases near wall and after some distance C increases in figure 19. On increasing time t in figures 23 and 24 it is observed that near wall temperature and concentration both decrease and after some distance from wall both temperature and concentration increase.

The numerical values of skin-friction coefficients τ_1 and τ_2 are presented in table-1. From table, we observe that on increasing dust particle parameter, dusty fluid parameter, inclination angle and Schmidt number skin-friction coefficients τ_1 and τ_2 both decrease. On the other hand skin-friction coefficients τ_1 and τ_2 increase as Hall parameter, viscoelastic parameter and Soret number increase. skin-friction coefficient τ_1 decreases as well as τ_2 increases when radiation parameter increases. skin-friction coefficient τ_1 increases as well as τ_2 decreases as Dufour number increases.

It is observed from table-2 Dufour number, Schmidt number and radiation parameter increase then Nusselt number Nu decrease and Sherwood number Sh increase. On other hand Soret number increases Nusselt number Nu increases and Sherwood number Sh decreases.

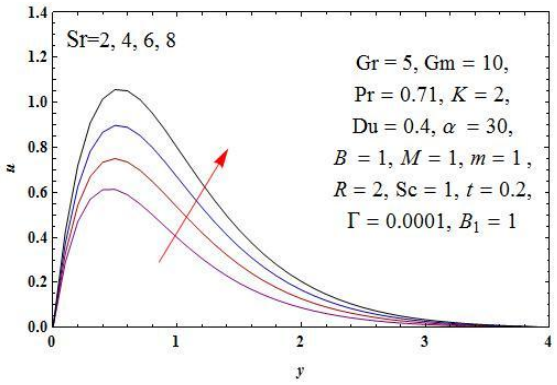

Fig. 1: Velocity Profile *u* for Different Values of *Sr*

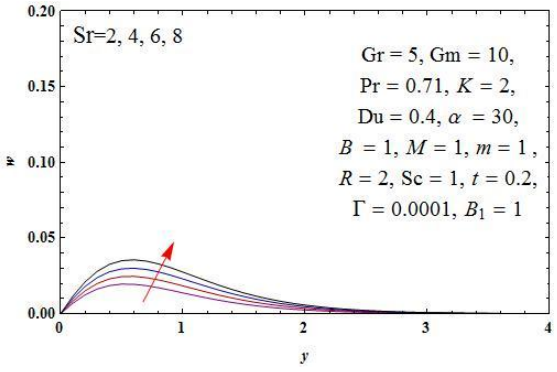

Fig. 2: Velocity Profile *w* for Different Values of *Sr*

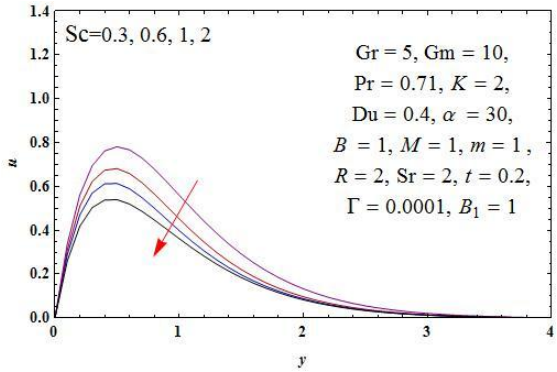

Fig. 3: Velocity Profile *u* for Different Values of *Sc*

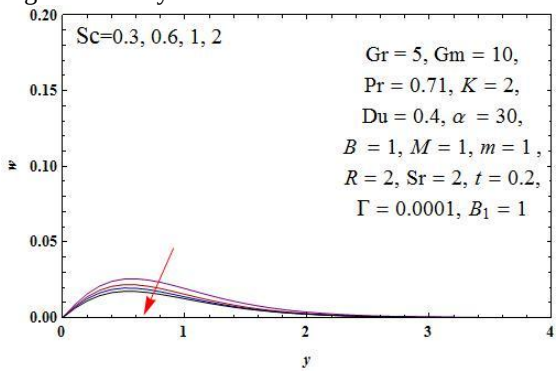

Fig. 4: Velocity Profile *w* for Different Values of *Sc*

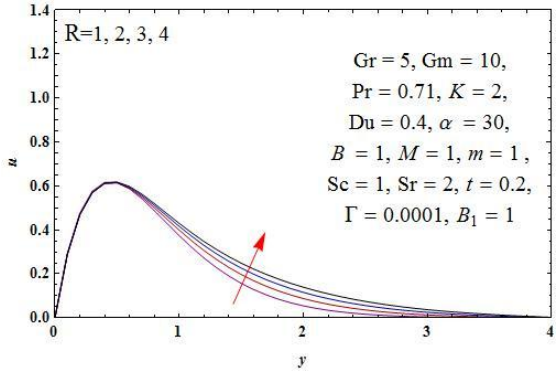

Fig. 5: Velocity Profile *u* for Different Values of *R*

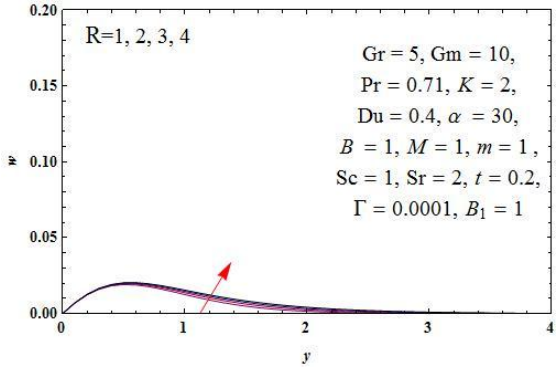

Fig. 6: Velocity Profile *w* for Different Values of *R*

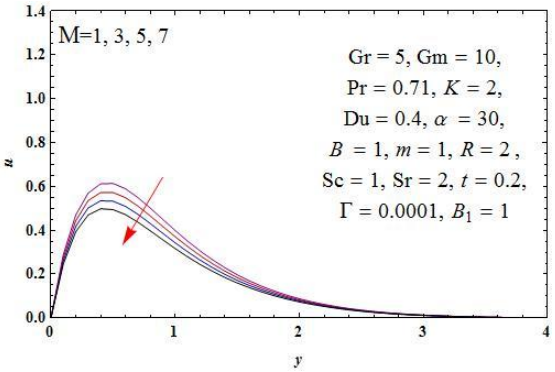

Fig. 7: Velocity Profile *u* for Different Values of *M*

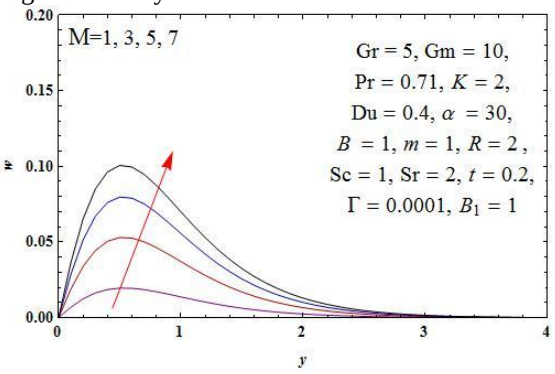

Fig. 8: Velocity Profile *w* for Different Values of *M*

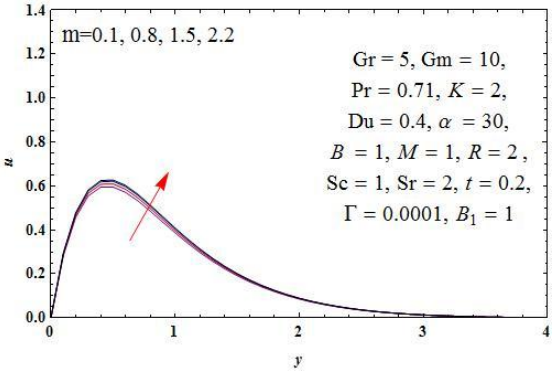

Fig. 9: Velocity Profile *u* for Different Values of *m*

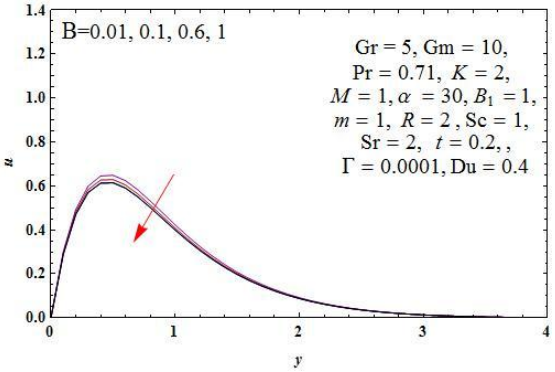

Fig. 10: Velocity Profile *u* for Different Values of *B*

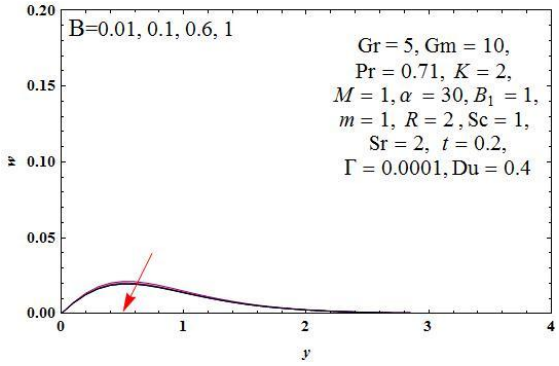

Fig. 11: Velocity Profile *w* for Different Values of *B*

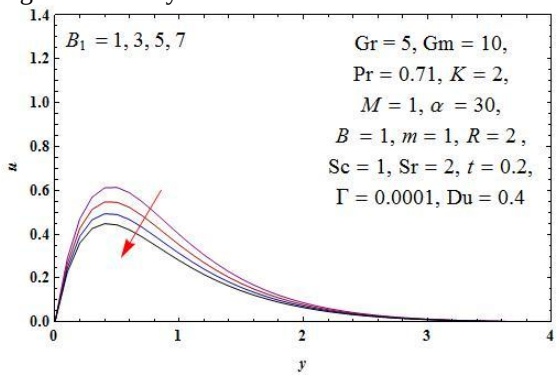

Fig. 12: Velocity Profile *vb*1 for Different Values of *B*1

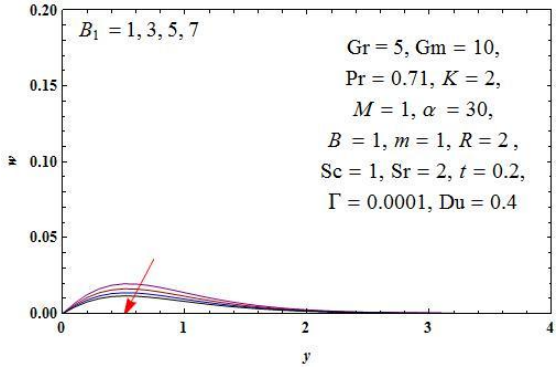

Fig. 13: Velocity Profile *w* for Different Values of *B*1

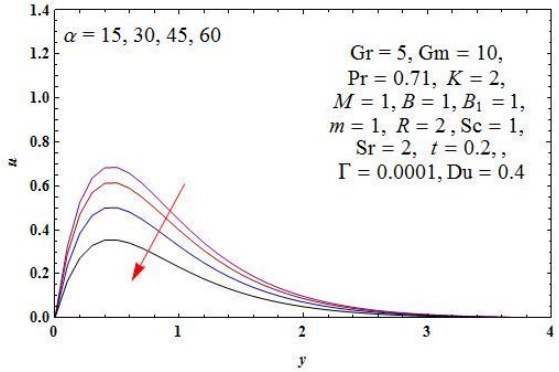

Fig. 14: Velocity Profile *u* for Different Values of _

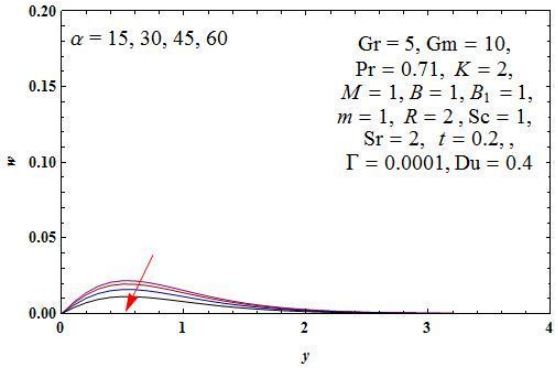

Fig. 15: Velocity Profile *w* for Different Values of _

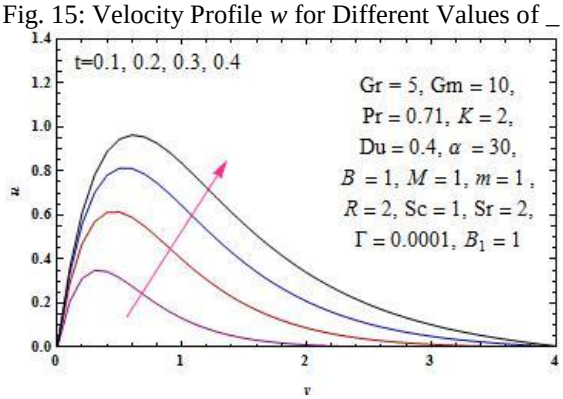

Fig. 16: Velocity Profile *u* for Different Values of *t*

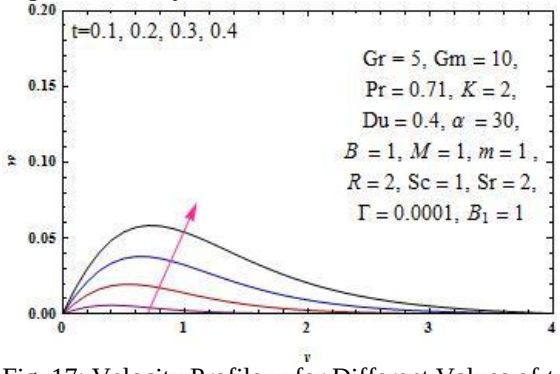

Fig. 17: Velocity Profile *w* for Different Values of *t*

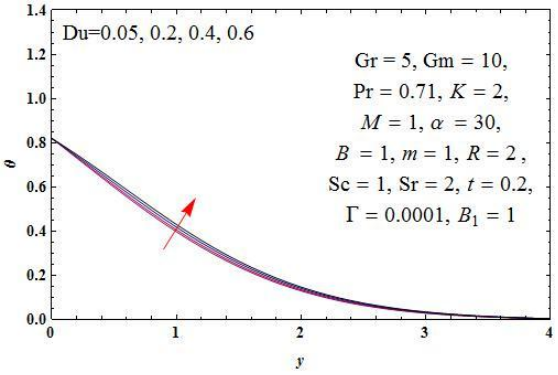

Fig. 18: Temperature Profile _ for Different Values of *Du*

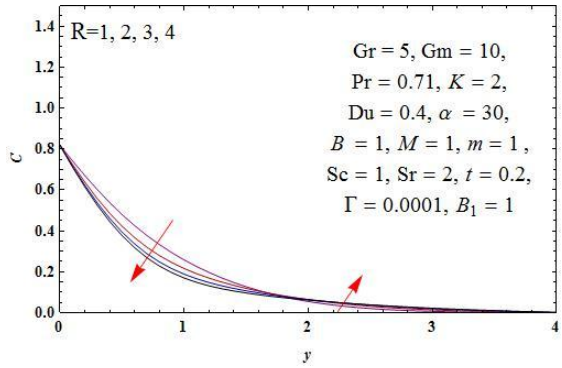

Fig. 19: Concentration Profile *C* for Different Values of *R*

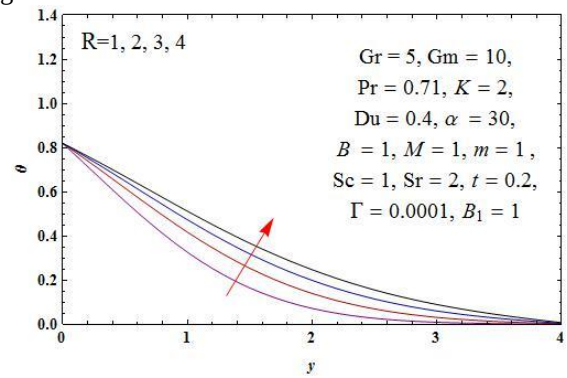

Fig. 20: Temperature Profile _ for Different Values of *R*

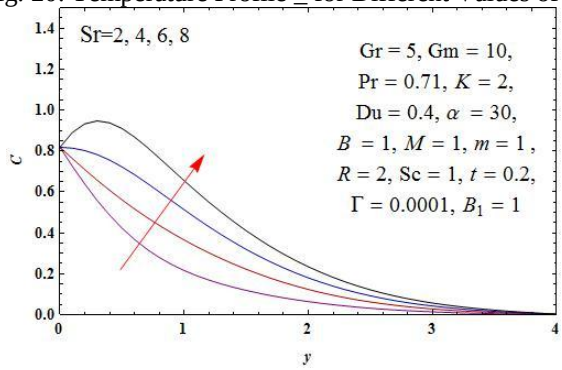

Fig. 21: Concentration Profile *C* for Different Values of *Sr*

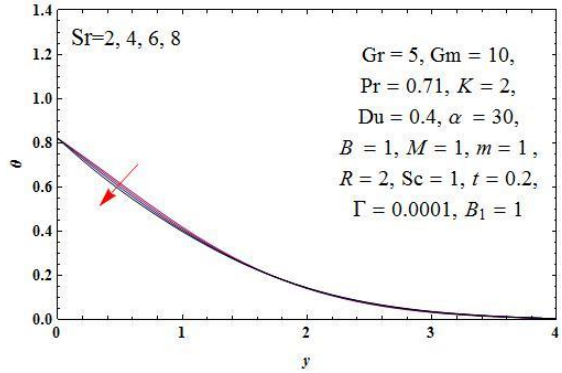

Fig. 22: Temperature Profile _ for Different Values of *Sr*

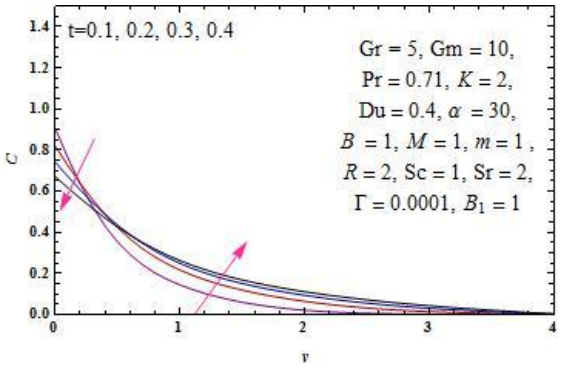

Fig. 23: Concentration Profile *C* for Different Values of *t*

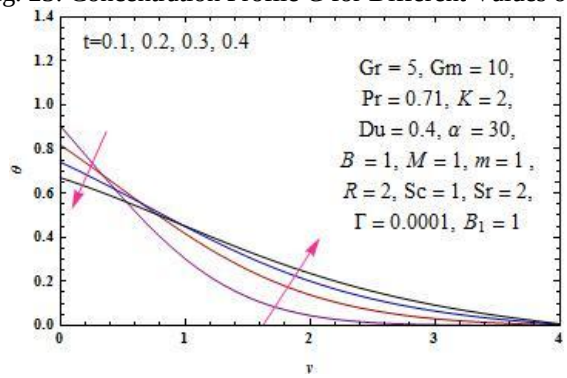

Fig. 24: Temperature Profile _ for Different Values of *t*

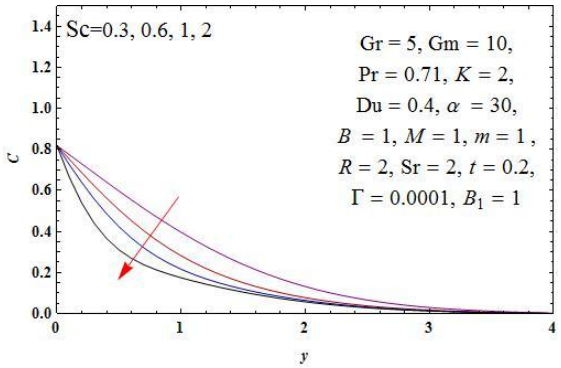

Fig. 25: Concentration Profile *C* for Different Values of *Sc*

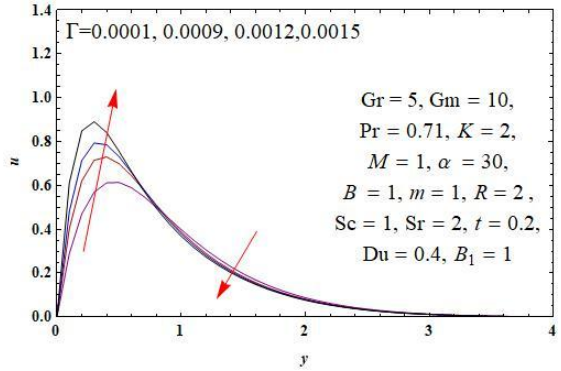

Fig. 26: Velocity Profile *u* for Different Values of Γ

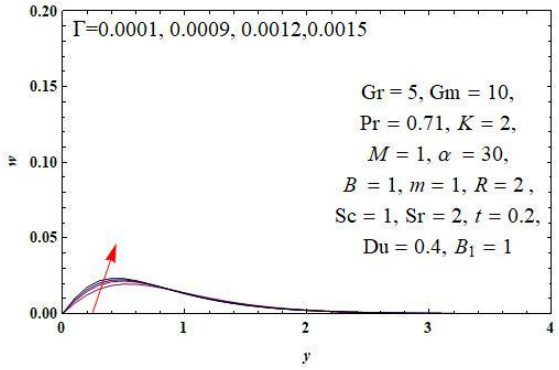

Fig. 27: Velocity Profile *w* for Different Values of Γ

V. CONCLUSION

The governing equations for unsteady MHD flow of dusty viscoelastic incompressible fluid over a inclined porous plate embedded in porous medium with Soret-Dufour, radiation effects in the presence of transverse magnetic field was formulated. The solutions for the model have been obtained by using Crank-Nicolson implicit finite difference method. The conclusions of the study are as follows:

1) The velocity u increases when dusty fluid parameter increases as well as velocity w also increases.
2) Concentration C decreses near plate and after some distance to plate it increses when radiation parameter increases.
3) Concentration C has major change near to plate when Soret number increases.
4) There is interesting result in velocities u and w when increase Soret number, we see that just near to plate for all values of parameter there is good buoyancy effect and after some distance there it is found normal change.

Table-1 Skin friction coefficients τ_1 and τ_2 for different values of parameters

Du	*Γ*	*B*	B_1	*R*	*M*	*m*	*Sc*	*Sr*	*α*	*t*	τ_1	τ_2
0.05	0.0001	1	1	2	1	1	1	2	30	0.2	2.90771	0.0691819
0.2	0.0001	1	1	2	1	1	1	2	30	0.2	2.90298	0.0691736
0.6	0.0001	1	1	2	1	1	1	2	30	0.2	2.88383	0.0691184
0.4	0.0009	1	1	2	1	1	1	2	30	0.2	4.02911	0.0832609
0.4	0.0012	1	1	2	1	1	1	2	30	0.2	4.81415	0.0912085
0.4	0.0015	1	1	2	1	1	1	2	30	0.2	6.11352	0.1021
0.4	0.0001	0.01	1	2	1	1	1	2	30	0.2	3.0193	0.0746572
0.4	0.0001	0.1	1	2	1	1	1	2	30	0.2	2.95464	0.0713422
0.4	0.0001	0.6	1	2	1	1	1	2	30	0.2	2.90023	0.0693746
0.4	0.0001	1	3	2	1	1	1	2	30	0.2	2.65393	0.0585005
0.4	0.0001	1	5	2	1	1	1	2	30	0.2	2.45129	0.0499247
0.4	0.0001	1	7	2	1	1	1	2	30	0.2	2.27836	0.0429684
0.4	0.0001	1	1	1	1	1	1	2	30	0.2	2.9253	0.0687585
0.4	0.0001	1	1	3	1	1	1	2	30	0.2	2.88533	0.0697664
0.4	0.0001	1	1	4	1	1	1	2	30	0.2	2.88483	0.0703953
0.4	0.0001	1	1	2	3	1	1	2	30	0.2	2.74681	0.188975
0.4	0.0001	1	1	2	5	1	1	2	30	0.2	2.60412	0.286691
0.4	0.0001	1	1	2	7	1	1	2	30	0.2	2.46713	0.365218
0.4	0.0001	1	1	2	1	0.1	1	2	30	0.2	2.82707	0.0131049
0.4	0.0001	1	1	2	1	0.8	1	2	30	0.2	2.8781	0.0667973
0.4	0.0001	1	1	2	1	1.5	1	2	30	0.2	2.92119	0.0649677
0.4	0.0001	1	1	2	1	2.2	1	2	30	0.2	2.94145	0.0649677
0.4	0.0001	1	1	2	1	1	0.3	2	30	0.2	3.37776	0.0865514

0.4	0.0001	1	1	2	1	1	0.6	2	30	0.2	3.10436	0.0760051
0.4	0.0001	1	1	2	1	1	2	1	30	0.2	2.6012	0.0615142
0.4	0.0001	1	1	2	1	1	1	4	30	0.2	3.28418	0.0834197
0.4	0.0001	1	1	2	1	1	1	6	30	0.2	3.72682	0.0987155
0.4	0.0001	1	1	2	1	1	1	8	30	0.2	4.24291	0.115276
0.4	0.0001	1	1	2	1	1	1	2	15	0.2	3.22726	0.0771296
0.4	0.0001	1	1	2	1	1	1	2	45	0.2	2.36252	0.0564628
0.4	0.0001	1	1	2	1	1	1	2	60	0.2	1.67055	0.0399252
0.4	0.0001	1	1	2	1	1	1	2	30	0.1	2.07556	0.0263169
0.4	0.0001	1	1	2	1	1	1	2	30	0.3	3.33608	0.115328
0.4	0.0001	1	1	2	1	1	1	2	30	0.4	3.5763	0.160296

Table-2 Nusselt number and Sherwood number Nu and Sh respectively for different values of parameters

Du	***Γ***	***B***	***B_1***	***R***	***M***	***m***	***Sc***	***Sr***	***α***	***t***	***Nu***	***Sh***
0.05	0.0001	1	1	2	1	1	1	2	30	0.2	0.440289	0.856995
0.2	0.0001	1	1	2	1	1	1	2	30	0.2	0.420855	0.88549
0.6	0.0001	1	1	2	1	1	1	2	30	0.2	0.359525	0.97767
0.4	0.0009	1	1	2	1	1	1	2	30	0.2	0.392141	0.928242
0.4	0.0012	1	1	2	1	1	1	2	30	0.2	0.392141	0.928242
0.4	0.0015	1	1	2	1	1	1	2	30	0.2	0.392141	0.928242
0.4	0.0001	1	1	1	1	1	1	2	30	0.2	0.522893	0.754965
0.4	0.0001	1	1	3	1	1	1	2	30	0.2	0.327144	1.00505
0.4	0.0001	1	1	4	1	1	1	2	30	0.2	0.286627	1.04896
0.4	0.0001	1	1	2	3	1	1	2	30	0.2	0.392141	0.928242
0.4	0.0001	1	1	2	5	1	1	2	30	0.2	0.392141	0.928242
0.4	0.0001	1	1	2	7	1	1	2	30	0.2	0.392141	0.928242
0.4	0.0001	1	1	2	1	0.1	1	2	30	0.2	0.392141	0.928242
0.4	0.0001	1	1	2	1	0.8	1	2	30	0.2	0.392141	0.928242
0.4	0.0001	1	1	2	1	1.5	1	2	30	0.2	0.392141	0.928242
0.4	0.0001	1	1	2	1	2.2	1	2	30	0.2	0.392141	0.928242
0.4	0.0001	1	1	2	1	1	0.3	2	30	0.2	0.426168	0.443568
0.4	0.0001	1	1	2	1	1	0.6	2	30	0.2	0.41089	0.666976
0.4	0.0001	1	1	2	1	1	2	2	30	0.2	0.346615	1.54392
0.4	0.0001	1	1	2	1	1	1	4	30	0.2	0.418271	0.554122
0.4	0.0001	1	1	2	1	1	1	6	30	0.2	0.45458	0.0437638
0.4	0.0001	1	1	2	1	1	1	8	30	0.2	0.509812	-0.71856
0.4	0.0001	1	1	2	1	1	1	2	15	0.2	0.392141	0.928242
0.4	0.0001	1	1	2	1	1	1	2	45	0.2	0.392141	0.928242
0.4	0.0001	1	1	2	1	1	1	2	60	0.2	0.392141	0.928242
0.4	0.0001	1	1	2	1	1	1	2	30	0.1	0.651856	1.41094
0.4	0.0001	1	1	2	1	1	1	2	30	0.3	0.267512	0.688322
0.4	0.0001	1	1	2	1	1	1	2	30	0.4	0.19039	0.53439

References

[1]. K. Walters, Quart. J. Mech. Appl. Math. vol. 13, pp. 444, 1960.

[2]. G. C. Rana and V. Sharma,"Thermal Instability of a Walters'(Model B) Elastico-Viscous Fluid in the Presence of Variable Gravity Field and Rotation in Porous Medium", Journal of Non-Equilibrium Thermodynamics, vol. 26, no. 1, pp. 31-40, 2001.

[3]. S. Dholey, T Ray Mahapatra and A. S. Gupta, "Momentum and heat transfer in the magnetohydrodynamics stagnation point flow of a viscoelastic fluid towards a streching surfaces", Mechanica, vol. 42, no. 3, pp. 263-272, 2007.

[4]. N. Pandya and A. K. Shukla, "Effect of radiation and chemical reaction on an unsteady Walter's-B viscoelastic MHD flow past a vertical porous plate", Int. J. Adv. Appl. Math. and Mech., vol. 3, no. 3, pp. 19-26, 2016.

[5]. Pradeep Kumar, "Instability in Walters B' Viscoelastic Dusty Fluid through Porous Medium", Fluid Mechanics Research International Journal, vol. 1, no. 1, pp. 1-7, 2017.

[6]. T. R. Mahapatra and S.Sidui, "An analytical solution of MHD flow of two visco-elastic fluids over a sheet shrinking with quadratic velocity", Alexandria Engineering Journal, vol. 55, no. 1, pp. 163-168, 2016.
[7]. S.Jena, G. C. Dash and S. R. Mishra, "Chemical reaction effect on MHD viscoelastic fluid flow over a vertical stretching sheet with heat source/sink", Ain Shams Engineering Journal, 2016.
[8]. Manoj Kumar Nayak, Gauranga Charan Dash and Lambodar Prased Singh, "Heat and mass transfer effects on MHD viscoelastic fluid over a stretching sheet through porous medium in presence of chemical reaction", Propulsion and Power Research, vol. 5, no. 1, pp. 70-80, 2016.
[9]. N. Pandya and A. K. Shukla, "Effects of Thermophoresis, Dufour, Hall and Radiation on an Unsteady MHD flow past an Inclined Plate with Viscous Dissipation", International Journal of Mathematics and Scientific Computing, vol. 4, no. 2, pp. 79-87, 2014.
[10]. T. G. Cowling, Magnetohydrodynamics, Inter Science Publishers, New York, 1957.
[11]. Brice Carnahan, H. A. Luthor and J. O. Wilkes, Applied Numerical Methods, John Wiley and Sons, New York, 1969.

Authors Profile

Nidhi Pandya is Assistant Professor in Department of Mathematics, University of Lucknow,Lucknow and now a days she is working in viscous and viscoelastic fluids.

Ravi Kant Yadav is Research Scholar in Department of Mathematics , University of Lucknow and pursuing PhD degree from University of Lucknow,Lucknow. He is working in viscous and viscous elastic fluid in different channels and interfaces.